Three-Dimensional Printing: A Catalyst for a Changing Orthopaedic Landscape

Jonathan Minto, BA

Xuan Zhou, PhD

Jenna Osborn, MS

Lijie Grace Zhang, PhD

Kausik Sarkar, PhD

Raj D. Rao, MD

Investigation performed at the Department of Orthopaedic Surgery, George Washington University, Washington, DC

Abstract

» Three-dimensional (3D) printing is an emerging tool in provider and patient education, surgical planning, and the design and implementation of medical devices and implants.

» Recent decreases in the cost of 3D printers along with advances in and cost reduction of printable materials have elevated 3D printing within the medical device industry.

» The advantages of 3D printing over traditional means of implant manufacturing lie in its ability to use a wide array of materials, its fine control of the macro- and microarchitecture, and its unprecedented customizability.

» Barriers to the widespread adoption of 3D-printed implants include questions of implant durability, U.S. Food and Drug Administration (FDA) approval for patient-specific implants, and insurance coverage of those implants.

Orthopaedics is primed to take advantage of technologic advances in three-dimensional (3D) printing. Surgical instruments that have been developed with the latest technology, including patient-specific cutting jigs, guides, and templates, are currently in use, and initial data promise improved surgical accuracy and a reduction in operating room time. Three-dimensional-printed models tailored to patient-specific pathology improve surgical planning. Most exciting is the current research on and use of patient-specific implants and advancements in tissue engineering. Three-dimensional printing has an advantage over traditional means of manufacturing because of its ability to use a wide array of materials, its fine control of the macro- and microarchitecture, and its unprecedented customizability.

Three-dimensional printing, also known as additive manufacturing, has transformed segments of the medical device industry. Used originally for rapid prototype development, 3D printing is now making inroads into the manufacturing world. The hearing aid industry converted from conventional manufacturing techniques to 3D printing in <500 days, while firms that maintained traditional processes were unable to survive[1]. The expiration of several key patents has decreased the cost of 3D printers, and advances in and cost reduction of printable materials have driven much of the recent interest. In orthopaedic surgery, 3D printing is being studied and used for a variety of surgical applications[2] (Table I). Surgical instruments (e.g., patient-customized cutting jigs, templates, and guides) for knee arthroplasty, spinal surgery, and tumor resection currently are being used, and patient-specific implants and advancements in tissue engineering that are being investigated show

Disclosure: The authors indicated that no external funding was received for any aspect of this work. The **Disclosure of Potential Conflicts of Interest** forms are provided with the online version of the article (http://links.lww.com/JBJSREV/A541).

TABLE I Commercially Available Three-Dimensional-Printed Implants*

Company	Implant (Year of FDA Approval)	Method	Material
Stryker[119-123]	Tritanium PL (2016), Tritanium C (2017), Triathlon Tritanium (2017), and Tritanium TL (2018)	Laser rapid manufacturing (LRM) (a form of SLM)	Ti-6Al-4V
Zimmer Biomet[124,125]	Zyston Strut Open Titanium Spacer System (2018) and OsseoTi Foot and Ankle Reconstructive Wedges (2013)	Unspecified additive manufacturing process	Ti-6Al-4V
Johnson & Johnson Medical GmbH[126,127]	EIT Cellular Titanium Cervical Cage (2017), EIT Cellular Titanium PLIF Cage (2017), EIT Cellular Titanium TLIF Cage (2017), and EIT Cellular Titanium ALIF Cage (2017)	SLM	Ti-6Al-4V
Centinel Spine[128,129]	STALIF C FLX (2018), ACTILIF C FLX (2018), STALIF M FLX (2018), ACTILIF M FLX (2018), STALIF L FLX (2018), ACTILIF L FLX (2018), STALIF Lateral-Oblique FLX (2018), and ACTILIF Lateral-Oblique FLX (2018)	SLM	Ti-6Al-4V
Exactech[130,131]	Novation Crown Cup with InteGrip Acetabular Shell (2010)	EBM	Titanium alloy
Camber Spine[132,133]	SPIRA Open Matrix ALIF (2018) and ENZA-A Titanium ALIF (2018)	Unspecified additive manufacturing process	Ti-6Al-4V
Additive Orthopaedics[134-137]	Hammertoe System (2016), Foot and Ankle Wedge System (2016), Bunion Correction System (2017), and Locking Lattice Plates (2019)	Unspecified additive manufacturing process	Ti-6Al-4V
SI-BONE[138,139]	iFuse-3D (2017)	EBM	Ti-6Al-4V

*FDA = U.S. Food and Drug Administration, SLM = selective laser melting, and EBM = electron beam melting.

promise and the likelihood of immediate applicability[2-8].

Traditional implant manufacturing occurs through subtraction processes (e.g., milling, turning, and cutting), where a larger block of material is cut down to the desired shape and size, or through forming methods, where the material is reshaped (e.g., rolling, extrusion, and forging) without adding or removing material. Three-dimensional printing allows instruments and implants of predesigned shapes to be manufactured by sequential layered deposition of the selected material. While traditional manufacturing techniques generate randomly organized macropores[9], 3D printing allows for an intentional organization of implant microarchitecture with intentional design of pore size, pore number, and pore interconnectivity[9,10], regulating the elastic modulus and facilitating biointegration.

Bioprinting utilizes 3D-printing technologies to manufacture and assemble scaffolds, tissues, and cells in a precise layer-by-layer fashion to replace or repair native tissue[11]. Scaffold matrices that are created from natural or synthetic materials are seeded or directly printed with factors or cells that will drive tissue growth and regeneration[12]. In vitro and in vivo studies have shown the efficacy of bioprinted scaffolds for facilitating chondrogenesis and repair[13]. Cell-laden matrices have been constructed to induce cartilage regrowth and subchondral repair, but the zonal distribution of cartilage has been difficult to replicate[13,14]. Three-dimensional bioprinting utilizing precise control of microarchitecture has shown the potential to better replicate some of the complexity of native cartilage[13]. The primary difficulty faced in the development of this technology is vascularizing implanted tissue[5,11]. Tissue that is >200 μm thick is beyond the diffusion depth of oxygen and requires a vascular network to survive[5,11].

This review article aims to provide a scientific overview of 3D printing, including the manufacturing process, the biologic and nonbiologic materials that are used and their relative benefits, implant architecture and durability, and the current clinical applications of 3D printing in orthopaedics.

Three-Dimensional Printing

Three-dimensional printing is a group of processes that creates objects from 3D modeling layer by layer. The first step is to produce a 3D image. Computed tomography (CT) is the most common imaging modality that is used to construct the 3D model[15,16]. Three-dimensional printers require the target object to have a discrete region that is enclosed by defined surfaces, something that DICOM (Digital Imaging and Communications in Medicine) images from CT scans do not provide[16]. Raw DICOM images are used to create a standard tessellation language (STL) file or an additive manufacturing file (AMF) that defines regions for the 3D printer[16]. The STL format does this by encompassing the "region" in interlocking triangular facets[16]. The newer AMF format was created to provide a more complete format by integrating more granular details such as color, texture, or differences in material[16]. The slice thickness of the image is critical for constructing appropriate spatial resolution, and 1.25 mm is the cutoff for creating a smooth construct[15].

Specific computer-aided design (CAD) software paired with an expert operator can achieve an overall accuracy in relation to the segmented anatomy of <1 mm or <3%[15]. Contemporary clinical imaging is typically done at ultrahigh spatial resolutions of 400 to 600 μm, with a slice thickness of <1 mm[15].

Three-dimensional printing of the product is carried out after the virtual model has been constructed. There are several printing processes, which are broadly based on extrusion, powder polymerization, sintering, or droplet spraying (Table II). Cost, post-processing, sterilization, printable materials, multi-material printing, and printing resolution and time are all considerations when choosing a printing method. Electron beam melting (EBM) and selective laser melting (SLM) are the 2 main printing methods that are used to create metal orthopaedic implants[16]. Generally, fused deposition molding (FDM) has been used to fabricate biomimetic tissue (bone, liver, and cartilage)[17,18]. Bioplotting and stereolithography (SLA) have been employed to print soft tissue (cartilage and blood vessels)[19-24]. Selective laser sintering (SLS) can create hard (metal/ceramic) supportive scaffolds with a hierarchical structure for implantation[25-27]. Inkjet printing has been utilized to prepare organ-on-chip designs, which are microfluidic devices that are aimed at providing a controlled microenvironment for living cells[28,29].

Materials That Are Used in 3D Printing

Three-dimensional-printed orthopaedic implants are directed toward supporting or replacing bone or cartilage. Two broad categories of material are used in 3D printing: inorganic materials and biomaterials. Inorganic materials include thermoplastics, photopolymers, metals (including titanium and its alloys), and polyesters (including polyetheretherketone [PEEK] and its composites). Thermoplastics are plastic polymers that are used in medical models for education or planning a complex surgical approach or procedure. Bioinks use biomaterials, either natural or synthetic, combined with live cells to promote tissue regeneration[30]. Natural biomaterials are polymers that are derived from organic resources, and, as a class, they provide better biocompatibility, biodegradability, and self-assembling abilities compared with synthetics[31]. Examples include agarose, alginate, collagen, and hyaluronic acid (HA). Synthetic biomaterials include polyethylene glycol (PEG); Pluronic (BASF), a nonionic detergent; methacrylated HA (HAMA) combined with thermosensitive hydrogels; allyl-functionalized poly(glycidol)s cross-linked with thiol-functionalized HA; and polyvinylpyrrolidone (PVP)[30-34]. Synthetics provide mechanical stability and good

TABLE II Common Three-Dimensional-Printing Technologies*

Process	Name	Mechanics	Advantages/Disadvantages	Bioprinting Materials	Potential Application
Extrusion-based	Fused deposition modeling (FDM)[17,18]	Filaments are extruded through a heated nozzle and deposited in predesigned form	Can use several materials in 1 structure; slow print speed and medium resolution (~100 μm); and medium mechanical strength	Thermoplastic filament/copolymer (PLA, ABS, PVA, PET, TPU)	Used for lungs, liver tissue, bone, cartilage, and osteochondral tissue printing
	Bioplotting/direct ink writing[19,20]	Inks and cross-linker are simultaneously extruded through a nozzle, and then cross-linked	Can use several bioinks in 1 structure; cell-laden inks are available; medium print speed; medium resolution (~100 μm); and low mechanical strength	Polymer and biomacromolecule (alginate, gelatin, Matrigel (Corning), hyaluronic acid)	Soft tissue (blood vessels, lungs, liver)/cartilage printing
Polymerization-based	Stereolithography (SLA) or digital light processing (DLP)[21-24]	Polymer resins photopolymerized by laser/digital light	Can use several bioinks in 1 structure; cell- laden inks are available; fast print speed; high resolution (~2 μm); and low mechanical strength	Photopolymer resin and biomacromolecule (alginate, gelatin, Matrigel, hyaluronic acid)	Soft tissue (blood vessels, lungs, liver)/cartilage printing
Sintering-based	Selective laser sintering (SLS), selective laser melting (SLM), electron beam melting (EBM), and direct metal laser sintering (DMLS)[25-27,132]	Powders heated by high-energy laser and deposited in required shape	Can use 1 ceramic/metal powder in 1 structure; slow print speed; low resolution (~2 mm); and high mechanical strength	Thermoplastic/ceramic/metal powder	Complex supportive scaffold (metal/ceramic implantation)
Droplet-based	Inkjet printing[28,29]	Droplets sprayed onto platform where they cure in desired shape	Can use several bioinks in 1 structure; cell- laden inks available; printing condition restriction; fast print speed; high resolution (~2 μm); and low mechanical strength	Polymer and biomacromolecule (alginate, gelatin, Matrigel, hyaluronic acid)	Cell spheroid, organ-on-a-chip

*PLA = polylactic acid, ABS = acrylonitrile butadiene styrene, PVA = polyvinyl alcohol, PET = polyethylene terephthalate, and TPU = thermoplastic polyurethane.

printing resolution through their mechanical and cross-linking properties, but often are combined with natural biomaterials to enhance biocompatibility.

Implant Architecture

Traditional methods of manufacturing are limited to randomly generating microarchitecture[9]. Three-dimensional printing has the potential to create customized implants that maximize durability, tissue regeneration, and biointegration by precisely controlling the implant microarchitecture. By manipulating the porosity, the pore size, the pore shape, and the pore surface curvature, 3D printing can reproduce the mechanical properties of tissue and minimize associated drawbacks[35].

Implant porosity establishes the architecture that is necessary for capillary growth and nutrient transportation, and increases the surface area that is available for tissue regeneration and fixation[36]. Altering porosity also changes the elastic modulus in order to develop implants that are more consistent with cortical or cancellous bone, reduce stress-shielding, and reduce cortical atrophy of adjacent bone[36]. However, increasing the porosity and decreasing the elastic modulus can lead to implant instability, deformation, and failure[37,38]. Implant porosity is directly related to pore size and pore interconnectivity. A minimum pore size of 100 μm is necessary for tissue regeneration, and pores sizes that are >300 μm are recommended because of increased capillary formation and bone regeneration[39]. Three-dimensional printing can similarly replicate the zonal microarchitecture of cartilage. Cartilage consists of 3 zones: superficial, transitional, and deep. These zones vary in extracellular matrix (ECM), cell organization, and zone-specific cell markers[14]. It has been theorized that mimicking this zonal architecture will improve implant integration and performance[32,40].

Individual pore shape can vary among simple geometries (e.g., cubes to more complex shapes). Variability in the pore surface, specifically the degree of surface curvature and the type of curvature, has been shown to influence the rate of tissue regeneration. The degree of curvature demonstrates a proportional relationship to the rate of tissue regeneration, with mean curvatures of 0° being closest to the mean curvature of trabecular bone[40,41]. Concave surfaces elicit an increased degree of tissue growth, and growth decreases on convex surfaces[42]. Therefore, concave and convex surfaces can be used to direct tissue growth, effectively customizing where and to what degree biointegration occurs.

Bone

Implants that are designed to repair or replace bone typically are made from titanium alloys or polyesters. Titanium provides an excellent strength-to-weight ratio, biocompatibility, biointegration, durability, a lower elastic modulus than stainless steel, and good corrosive resistance. Concerns with titanium implants are related primarily to their higher modulus of elasticity, which can lead to adjacent bone resorption, metal distortion on magnetic resonance imaging (MRI), and the potential for long-term periprosthetic osteolysis[43,44]. PEEK and its composites are an increasingly popular material choice, with durability and biocompatibility that are suitable for weight-bearing implants (a modulus of elasticity similar to cortical bone, 8.3 versus 17.7 GPa), and they do not have the MRI incompatibility or hypersensitivity concerns of metallic implants[44-46]. The smooth surface of PEEK prevents tissue binding, thus rendering it biologically inert[44]. Surface treatment or composite preparation can increase implant biointegration and include physical or chemical roughening, or coating with bioactive substances such as calcium phosphate or HA[44]. An example of composite preparation is an HA/PEEK composite that combines a bioactive substance, HA, with PEEK[44,46].

Three-dimensional-printed bioinks that are used in bone-tissue engineering have shown promise in producing new bone[47,48]. Vascularization is an essential step in order for a large 3D-bioprinted bone to be functional. One study that used a cell-laden hydrogel mixture of poly(ε-caprolactone) (PCL) polymer, tricalcium phosphate (TCP), and poloxamer 407 with a poloxamer 407 support scaffold produced vascularized bone tissue[48]. Several studies have produced 3D-bioprinted biphasic artificial vascularized bone composites with well-organized vascular networks[49-52]. The construct consisted of a supportive scaffold (polylactide [PLA] fibers) and cell-laden microvascularized gelatin methacrylate (GelMA) hydrogels. Bioactive factors, such as bone morphogenetic protein-2 (BMP-2) and vascular endothelial growth factor (VEGF) peptides, were introduced into the construct to promote both osteogenesis and angiogenesis (Fig. 1). Cui et al. designed a novel 3D-printed vascularized bone tissue with a biologically inspired smart growth-factor release system[51] (Fig. 2). They demonstrated the formation of well-organized vascularized bone tissue with excellent osteogenic potential, based on type-I collagen expression and calcium content.

Cartilage

Unlike bone, native cartilage has poor regenerative capacity because of its avascularity and complex architecture[53]. Three-dimensional-bioprinting technology demonstrates promise in fabricating customized artificial constructs of cartilage tissue[13]. Cartilage bioink usually uses a hydrogel that is seeded with biologically active chondrogenic cells. Autologous chondrocytes are the most frequently used cells for cartilage implants[32,54-56], but multipotent mesenchymal stem cells (MSCs) that are capable of differentiating into chondrocyte-like cells also have been used[32,57]. Other chondroprogenitor cells and combinations of chondrocytes and MSCs have been explored as well[32,58-61]. An alternative to seeding a biomaterial with active cells is the incorporation of biostimulating materials, including growth factors, bioactive proteins, and matrix components, which attract host cells or stimulate

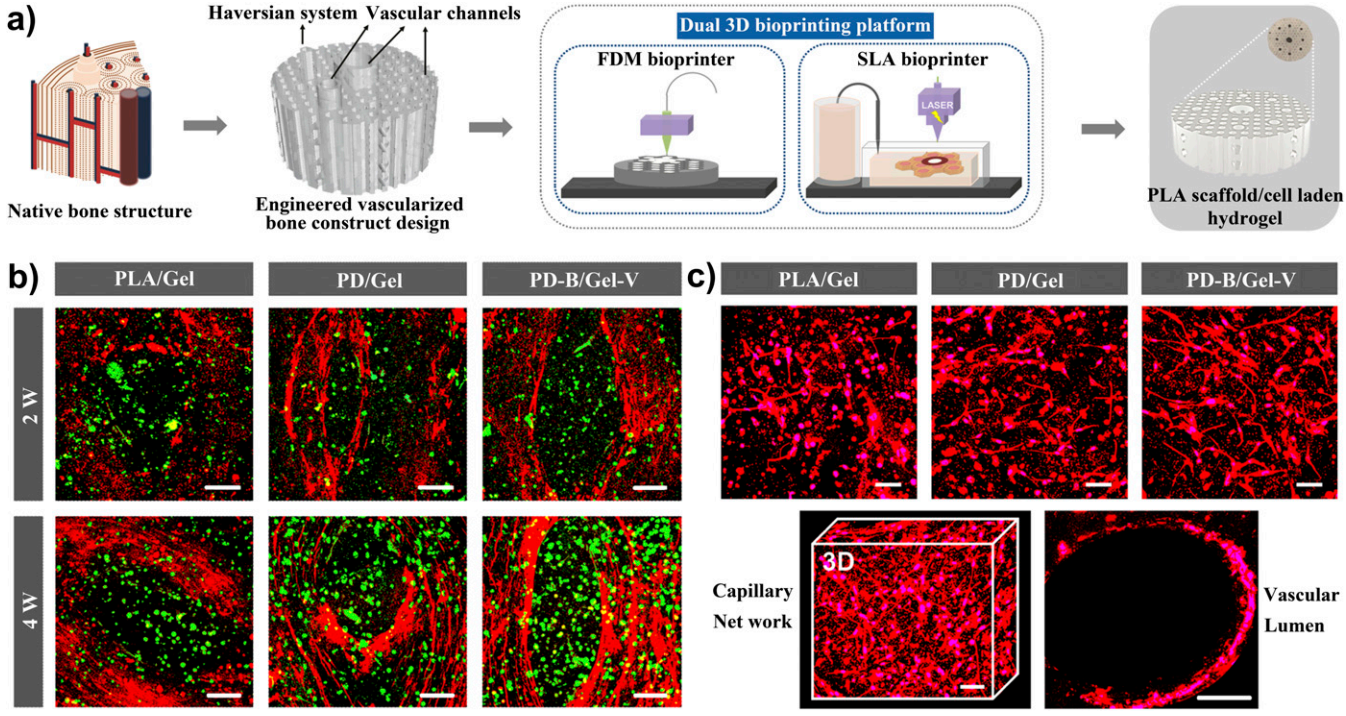

Fig. 1

Figs. 1-A, 1-B, and 1-C Schematic illustration and fluorescence images. FDM = fused deposition modeling, SLA = stereolithography, and PLA = polylactic acid. (Reproduced, with permission, from: Cui H, Zhu W, Nowicki M, Zhou X, Khademhosseini A, Zhang LG. Hierarchical fabrication of engineered vascularized bone biphasic constructs via dual 3D bioprinting: integrating regional bioactive factors into architectural design. Adv Healthc Mater. 2016 Sep;5[17]:2174-81. Epub 2016 Jul 7. © 2016 WILEY-VCH Verlag GmbH & Co. KGaA, Weinheim.) **Fig. 1-A** Schematic illustration of a 3D-bioprinted biphasic vascularized bone construct via a dual 3D-bioprinting platform. **Fig. 1-B** Immunofluorescence staining of the vascularized bone formation in the biphasic structural constructs. The fluorescence images for anti-von Willebrand factor (vWF, green) and osteopontin (OPN, red) show that the bioprinted construct with both bone morphogenetic protein-2 (BMP-2) and vascular endothelial growth factor (VEGF) (PD-B/Gel-V) possesses higher angiogenesis and osteogenesis than other control groups. The scale bars indicate 100 μm. **Fig. 1-C** Immunofluorescence staining of the vascular capillary network and lumen that were identified as positive for CD31 antibody in a 3D-bioprinted construct after 4 weeks. The scale bars indicate 50 μm.

them toward chondrogenesis[32,62]. Zhou et al. reported bioprinting a series of cartilage scaffolds using GelMA (polyethylene glycol diacrylate [PEGDA] ink graphene oxide [GO] nanoparticles) with an SLA printer[63]. The resulting cartilage tissue scaffolds demonstrated greater glycosaminoglycan (GAG) synthesis by the MSCs when compared with controls without nanoparticles.

Using 3D bioprinting, osteochondral tissues that integrate both cartilage and bone in a single construct have been created[64-67]. Castro et al. prepared 3D-printed biomimetic osteochondral scaffolds[65] (Fig. 3). The study found that nanoinks, bioinks that incorporate structures on the nanometer scale (e.g., nanopores or nanorods), greatly improve stem-cell adhesion and direct osteogenic and chondrogenic differentiation. In another study, Nowicki et al. utilized an FDM-based 3D printing system to fabricate investment-casting molds with varied pore distribution over the full thickness of the high-impact polystyrene scaffold[64]. The osteochondral scaffold exhibited good biologic and mechanical performance.

Recent studies have shown a possible role for mechanical cues in the growth and integration of bone and cartilage tissue. The alternating changes in tissue pressure from low-intensity pulsed ultrasound (LIPUS) have been hypothesized to induce micromechanical stresses, resulting in its previously demonstrated effects in fracture-healing[68-71], wound-healing[72], and the treatment of glaucoma[73]. In vitro experiments suggest that LIPUS treatments induce multifunctional effects that are linked with bone formation and resorption[74]. LIPUS enhances the proliferation of MSCs and their osteogenic[75] and chondrogenic[76] differentiation on 3D-printed tissue constructs (Figs. 4-C through 4-H)[76].

Microbubbles that are coated by a monolayer of lipids, proteins, or other surface-active molecules are strong reflectors of ultrasound[77-81]. LIPUS in the presence of lipid-coated microbubbles shows significantly enhanced chondrogenesis of MSCs on a 3D-printed PEGDA hydrogel scaffold. GAG production increased by 17% (5% by LIPUS alone) and type-II collagen production increased by 78% (44% by LIPUS alone)[82]. Similar enhancement of osteogenic differentiation of MSCs also was found in 3D-printed PLA scaffolds, and the enhancement was larger than when LIPUS was used alone (Figs. 4-A through 4-E)[83].

Durability

The lack of assurance on the biomechanical durability of 3D-printed metal

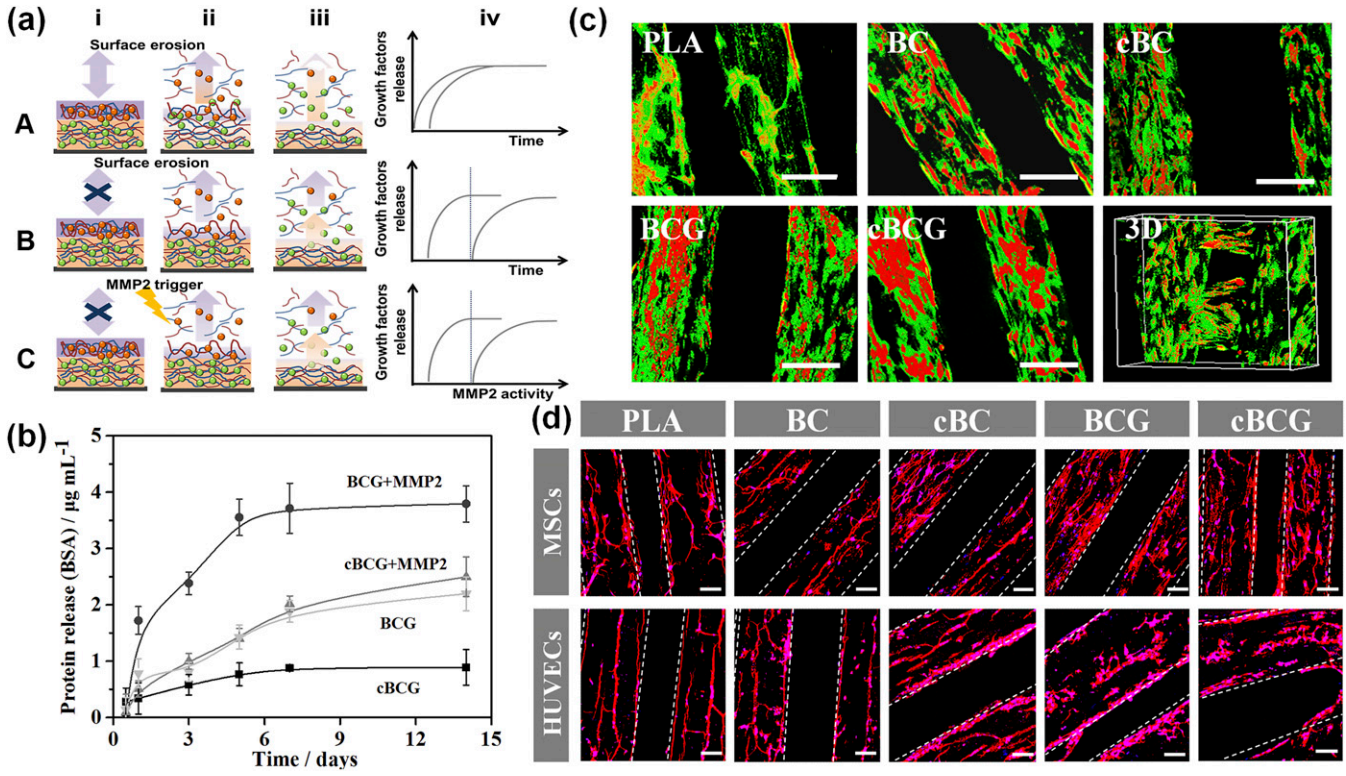

Fig. 2

Figs. 2-A through 2-D Illustrations and fluorescence images. BSA = bovine serum albumin, BC = bioactive nanocoating (Gel/poly-L-lysine $[PLL]_{20}$)-modified PLA, BCG = bioactive nanocoating with growth factors, cBC = Genepin (Gnp) cross-linked bioactive nanocoating $[(Gel/PLL)_{20}]$ Gnp-modified PLA, cBCG = Gnp-cross-linked bioactive nanocoating with growth factors, and PLA = polylactic acid. (Reproduced, under Open Access license CC BY 4.0, from: Cui H, Zhu W, Holmes B, Zhang LG. Biologically inspired smart release system based on 3D bioprinted perfused scaffold for vascularized tissue regeneration. Adv Sci (Weinh). 2016 Apr 15;3[8]:1600058. © 2016 The Authors. Published by WILEY-VCH Verlag GmbH & Co. KGaA, Weinheim.) **Fig. 2-A** Schematic illustration of a controllable smart bioactive factor release (C) in the 3D-bioprinted bone when compared with traditional layer-by-layer film absorption with surface erosion release mode (without [A] and with [B] cross-linking). The bone morphogenetic protein-2 (BMP-2) (green spheres) and vascular endothelial growth factor (VEGF) (red spheres) are loaded into films composed of polylysine (blue) and matrix metalloproteinase (MMP) trigger-cleavable gel (red). **Fig. 2-B** Protein release profiles of nanocoating with bovine serum proteins within 2 weeks. **Fig. 2-C** Confocal microscopy images of human bone marrow mesenchymal stem cells (MSCs, green) and human umbilical vein endothelial cells (HUVECs, red) cocultured on various scaffolds for 5 days. The scale bars are 200 μm. **Fig. 2-D** Fluorescence microscopy images of MSCs and HUVECs on the 3D-bioprinted vascularized bone scaffolds with F-actin (red) and nucleus (blue) staining for 3 days. The MSCs had a well-distributed spread on the scaffold surface, while the HUVECs formed aggregative microvascular networks. The scale bars are 100 μm.

implants, when compared with traditional manufacturing techniques, is a hurdle to their widespread clinical adoption. Internal defects, porosity, residual stresses, and surface topography can all contribute to implant fatigue and failure in both wrought and 3D-printed materials[84,85]. The National Institute for Standards and Technology (NIST), a branch of the U.S. Department of Commerce, has established standards for assessing the durability of traditionally wrought materials by using guidelines set forth by ASTM International[86]. Additionally, NIST has a separate set of guidelines for assessing 3D-printed materials[87]. It recommends testing deformation properties (tension, compression, bearing yield strength, modulus, and hardness) and failure properties (fatigue, fracture toughness, and crack growth)[87]. Commercially available 3D-printed implants are expected to meet the same standards as traditionally manufactured implants to achieve U.S. Food and Drug Administration (FDA) approval[88]. Cyclic tension and compression stresses are recommended to replicate the in vivo stresses that are most likely to result in implant failure[89].

SLM and EBM metal implants have a natural rough surface when initially crafted[90]. This rough surface of as-built materials, materials that have not undergone post-processing surface treatments, provides crack initiation sites that can contribute to reduced fatigue resistance in SLM or EBM-made materials[90]. Although 3D-printed materials that are crafted with SLM or EBM initially show shortened fatigue lives when compared with wrought materials, early testing shows that parity can be achieved with the addition of post-processing surface or heat treatments, which can increase the fatigue resistance of SLM or EBM-made materials[90].

Although early clinical outcomes have been positive, long-term data can highlight concerning signs that may predict future failure of 3D-printed commercial implants. Early data from 109 hip replacement operations using the 3D-printed Stryker Tritanium acetabular cup in 95 patients showed a 98% survival rate at an average of 4.24 + 1.49

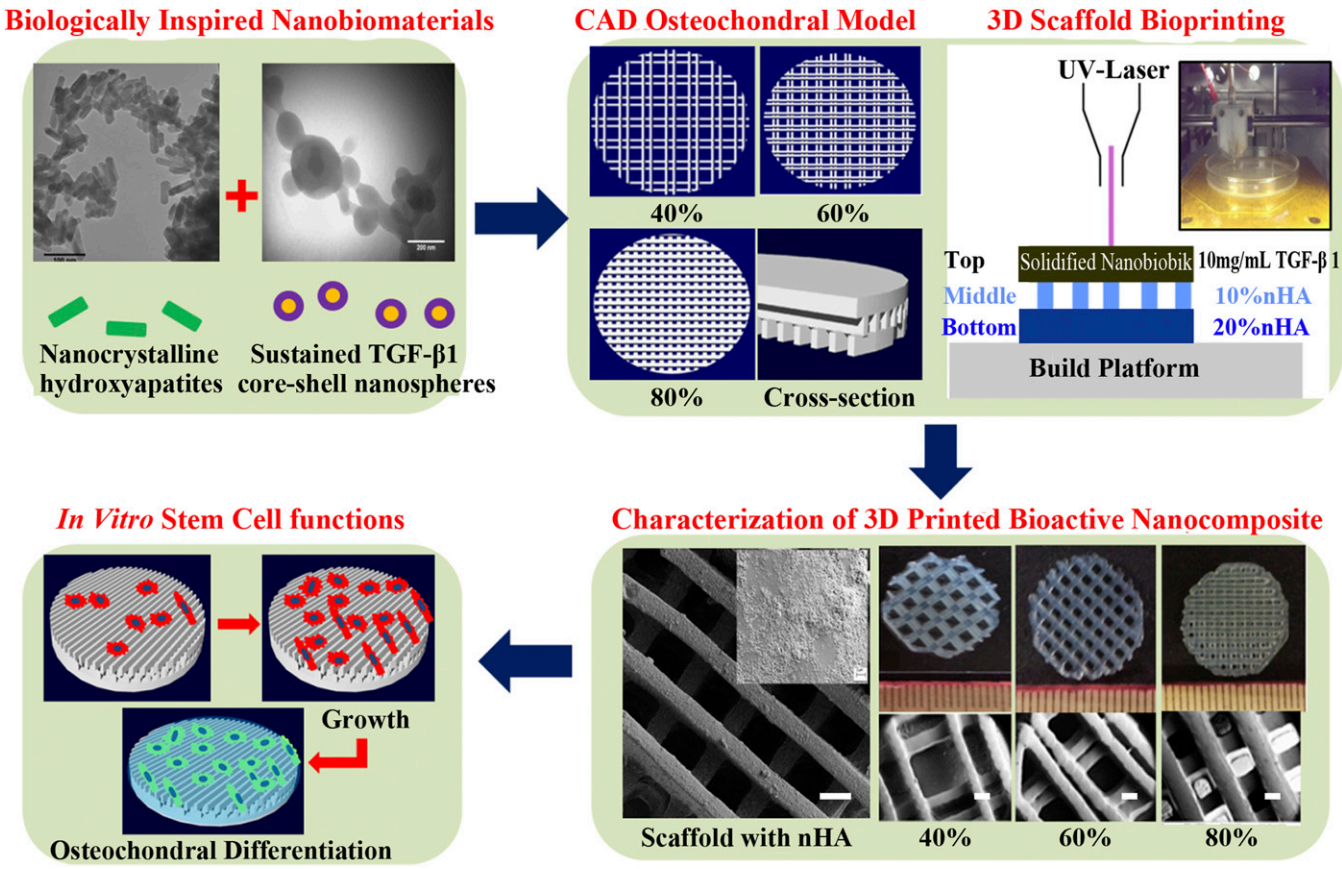

Fig. 3

Overview of 3D printing of a biomimetic nanocomposite osteochondral scaffold. UV = ultraviolet. *Top left:* tissue-specific nanobiomaterial-based printing inks for osteogenic (nHA = nano-hydroxyapatite) and chondrogenic (transforming growth factor [TGF]-β1-loaded core-shell nanospheres) differentiation of mesenchymal stem cells (MSCs). *Top right:* Computer-aided design (CAD) models of porous scaffold design and composition. *Bottom left:* Scanning electron microscopy and photographic images of the fabricated scaffolds with different porosities. *Bottom right:* an in vitro MSC function study. (Republished with permission of the Royal Society of Chemistry [Great Britain], from: Integrating biologically inspired nanomaterials and table-top stereolithography for 3D printed biomimetic osteochondral scaffolds. Castro NJ, O'Brien J, Zhang LG. Nanoscale. 2015 Sep 7;7[33]: 14010-22; permission conveyed through Copyright Clearance Center, Inc.)

years. Radiographs at 1 year demonstrated a 30.3% incidence of radiolucency in 2 DeLee zones and an 8.2% incidence in 3 zones[91]. At 5 years, this incidence jumped to 40.0% and 17.1%, respectively[91]. Another study retrospectively compared the same Stryker cup to the Stryker Trident cup, manufactured by traditional means, with two 130-patient cohorts[92]. That study showed increased radiolucent lines in the Tritanium cup (36.1% at 3 months and 60.7% at the time of final follow-up [41.3 months]) and decreased radiolucent lines in the Trident cup (2.5% at 3 months and 0.8% at the time of final follow-up [38.1 months])[92].

Metal implants generally are designed to remain permanently in the body, whereas 3D-printed biodegradable tissue scaffolds are designed to be degraded and replaced over time by native tissue; the intended durability depends on the materials that are used and the specific clinical function of the implanted tissue. Xu et al. implanted a 3D-printed PCL/hydroxyapatite scaffold into a long-bone defect in a goat. New bone formation occurred in the scaffold at 4 weeks postimplantation, and the scaffold was entirely replaced by new bone tissue at 12 weeks postimplantation[18]. In a study of 5 patients with 3D-printed metallic mandibular implants, Mangano et al. reported preserved function and alignment after 2 years of loading[26].

Orthopaedic Surgical Guides/Models

Three-dimensional-printed models based on individual patient imaging can mimic complex anatomy and unusual clinical circumstances, and do so in an affordable fashion. Surgical planning with these models allows a surgeon to preoperatively recognize challenges that may be encountered with a specific patient's anatomy and to develop surgical strategy, reduce operating room time, and improve patient outcomes[2,93]. Some authors have shown that less-experienced surgeons may benefit the most by using 3D models to preoperatively assess, plan, and practice[93].

Patient-specific instrumentation (PSI) in the form of intraoperative guide templates and jigs utilizes preoperative images to construct a 3D physical mold that fits over the surgical site. Slits and holes that are designed into the mold direct surgical instrumentation and facilitate

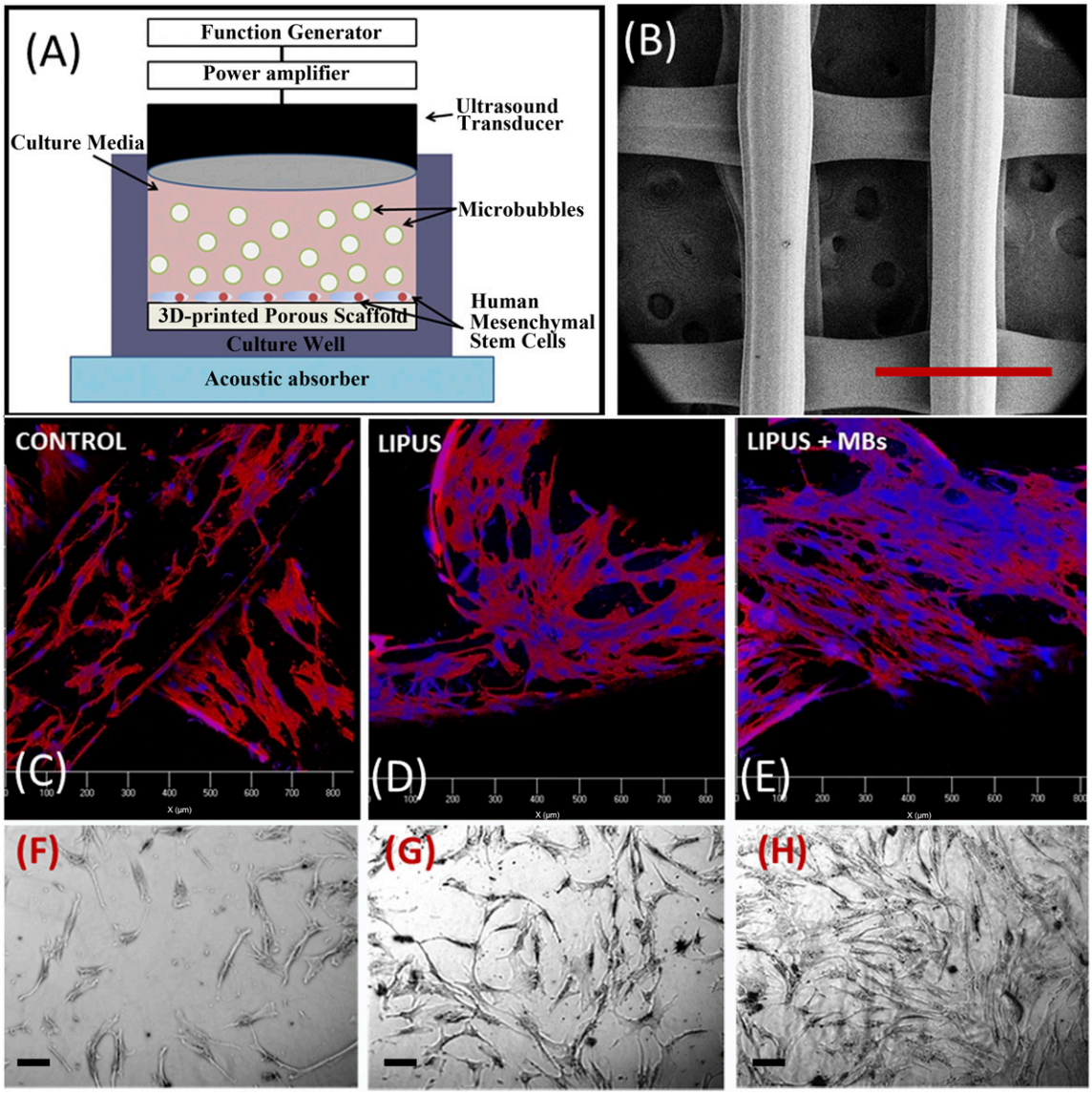

Fig. 4

Figs. 4-A through 4-H Three-dimensional-printed scaffolds, confocal images, and microscopic images. **Fig. 4-A** The experimental setup of exposing 3D-printed scaffolds and stem cells to low-intensity pulsed ultrasound (LIPUS) with and without microbubbles (MBs) present. **Fig. 4-B** Three-dimensional-printed polylactic acid (PLA) scaffolds used in experiments by Osborn et al.[83] (red scale bar = 1 mm). **Figs. 4-C, 4-D, and 4-E** Confocal images of mesenchymal stem cells seeded on PLA scaffolds after 3 days of culture in an osteogenic media (cytoskeleton and cell nuclei stained using Texas Red-X phalloidin [red] and DAPI [4′,6-diamidino-2-phenylindole] [blue]). **Fig. 4-C** control (no LIPUS or MBs). **Fig. 4-D** LIPUS stimulation. **Fig. 4-E** LIPUS stimulation with the presence of MBs. (Figs. 4-A through 4-E are reproduced, with permission, from: Osborn J, Aliabouzar M, Zhou X, Rao R, Zhang LG, Sarkar K. Enhanced osteogenic differentiation of human mesenchymal stem cells using microbubbles and low intensity pulsed ultrasound on 3D printed scaffolds. Adv Biosys. 2019;3(2):1800257. © 2018 WILEY-VCH Verlag GmbH & Co. KGaA, Weinheim.) **Figs. 4-F, 4-G, and 4-H** Microscopic images of mesenchymal stem cells after 5 days of culture in a chondrogenic media. (Reproduced, under Open Access license CC BY 4.0, from: Aliabouzar M, Zhang LG, Sarkar K. Lipid coated microbubbles and low intensity pulsed ultrasound enhance chondrogenesis of human mesenchymal stem cells in 3D printed scaffolds. Sci Rep. 2016 Nov 24;6:37728.) **Fig. 4-F** Control (no LIPUS or MBs). **Fig. 4-G** LIPUS stimulation. **Fig. 4-H** LIPUS stimulation with the presence of MBs.

implant navigation. In 1998, a 3D-printed PSI guide was utilized to improve the placement accuracy of spinal pedicle screws[94]. PSI guides have since been developed for additional clinical indications in the spine, the knee, the hip, and the shoulder, and with orthopaedic trauma surgeries, and some authors have shown modest increases in implant accuracy and reductions in operating room time[2,95].

Hip

Three-dimensional-printed PSI templates have been used as an alternative to conventional intraoperative computer assistance for central pin placement in the femoral neck during hip resurfacing. The drilling templates were as accurate as the computer-assisted techniques and had the same ease of use as the traditional mechanical guides[96].

Shoulder

Total shoulder arthroplasty outcomes are dependent on accurate glenoid component placement. In cases with severe glenoid arthritis and bone loss, or with surgeons who have limited intraoperative experience, 3D-printed patient-specific glenoid guides that have been used to direct the central glenoid guidewire have reduced the error of guide placement and improved the mean guidewire placement in both the vertical and horizontal planes[97].

Trauma

Three-dimensional-printed PSI has been used in orthopaedic trauma for osteotomy cutting guides of the radius and the tibial plateau and as a navigational guide for ankle ligament reconstruction[98-100].

Knee

A study using 3D-printed patient-specific cutting guides for femoral varization osteotomy showed precise limb correction, decreased operative time, and decreased time under fluoroscopy[101]. Malposition during unicompartmental knee arthroplasty can lead to early failure and to unequal wear. Patient-specific cutting blocks and guides have been used to improve the accuracy of such cases[102,103].

Spine

PSI has been utilized in the stabilization of the cervical spine for subaxial pedicle screw and C2 laminar screw placement. In a comparison of 4 methods (landmarks, fluoroscopy, image-guided surgery, and PSI) for inserting cervical pedicle screws, the use of landmarks resulted in inaccuracy rates as high as 87.5%. Fluoroscopy, which is the gold standard, was roughly 85% to 91% accurate. Image-guided surgery had good accuracy (76% to 97%) but was expensive and had a high learning curve. PSI was 80.6% to 100% accurate, had a low learning curve, required less radiation exposure, and reduced operating room time when compared with fluoroscopy[104,105]. Some benefit has been reported using PSI for thoracic pedicle screw placement, but no benefit has been reported for lumbar screw placement[106].

Orthopaedic Implants

There are 2 broad uses for 3D printing in designing patient-specific metal implants: (1) scaled implants that resemble traditionally manufactured implants but are scaled or sized with 3D printing to be more suitable to an individual patient, and (2) customized implants, tailored to a specific patient's anatomic variations. The Stryker interbody fusion cages are an example of scaled implants. These cages are tailored in height, width, depth, and angle to better accommodate an individual without changing the general design of the implant[107]. Scaled implants currently represent the largest share of commercial in vivo 3D-printed patient-specific implants. Customized implants also have been used to treat patients with unique anatomic needs (e.g., for hemipelvis prosthetics following tumor resection, in complex cervical spine reconstruction, and in customized cages that are used in the reconstruction of acetabula with massive defects)[108-110]. Porous titanium metaphyseal cones have been created for total knee arthroplasty, porous femoral stems have been used for total hip arthroplasty, and prosthetic scaphoid replacements have been used for individuals with scaphoid bone loss due to osteonecrosis or highly comminuted fractures[111-113].

FDA Considerations

The FDA has been monitoring the increased clinical interest in 3D printing. In 2017, a public workshop entitled "Additive Manufacturing of Medical Devices: An Interactive Discussion on the Technical Considerations of 3D Printing" resulted in guidance to address this burgeoning field[114]. The FDA recommends that 3D-printed implants and devices meet the same standards as traditionally manufactured implants[114]. Additionally, the FDA recommends documentation of the starting material, the initial state of the material (including the particle size for solid materials and the viscosity for fluids), and the certificates of analysis for all materials that are used[114]. A 3D-printed product can be dependent on a single printer; therefore, adequate maintenance of machine calibration, parameters, and settings must be ensured[114]. If material is reused, documentation should describe the process by which it is reused and what monitoring is in place to determine if the reused material underwent any chemical changes[114]. Post-processing helps reduce implant fatigue failure, and the FDA recommends that these steps be documented to "include a discussion of the effects of post-processing on the materials used and the final device."[114]

Several scaled implants have attained FDA approval, including the Stryker vertebral cages, the Zimmer Biomet interbody spacers and ankle fusion systems, and the Additive Orthopaedics hammer toe and wedge osteotomy system[107,115,116]. Under prior FDA guidance, custom implants are exempt from premarket approval[114]. A custom implant, as defined by the FDA, must be made for the specific needs of a physician or be used for an individual patient "for the purpose of treating a sufficiently rare condition, such that conducting clinical investigations on such device would be impractical" and limits the number of such devices to ≤5 units per year[117]. It is important to note that the FDA has not yet provided specific guidance for 3D-printed biologic implants. Instead, these devices must adhere to the existing regulations for biologics that are provided through the Center for Biologics Evaluation and Research (CBER). Insurance coverage for 3D-printed devices generally follows FDA approval and medical necessity[118].

Overview

Three-dimensional printing represents a potential transformative force in orthopaedic surgery. The technology provides easy customization by

controlling the macro- and micro-architecture, and enabling precise control of the elastic modulus, porosity, and biointegration. A variety of materials are available, including metals, polyesters, and thermoplastics, which allow for further control over implant properties.

Three-dimensional-printed guides and templates can assist with difficult surgeries for inexperienced surgeons and reduce operative time, while models are beneficial for presurgical planning and patient education. Implants can be tailored to individual patient anatomy and pathology, providing solutions to patient-specific problems. Post-processing creates implants with durability similar to that of traditional manufacturing methods, but more long-term data are necessary to assess the durability of implants in patient-specific shapes. Scaled implants have received FDA approval, and may represent an early shift in the adoption of 3D printing for devices that require greater adjustability.

Bioprinting shows the potential to replace or repair lost bone or cartilage with printed tissue or regenerative constructs. A better understanding of implant vascularization and sterility and long-term in vivo data will help validate these implants. Increasing collaboration between scientists and clinicians will inevitably result in the safer and more widespread utilization of this versatile technology in orthopaedic applications.

Jonathan Minto, BA[1],
Xuan Zhou, PhD[2],
Jenna Osborn, MS[2],
Lijie Grace Zhang, PhD[2],
Kausik Sarkar, PhD[2],
Raj D. Rao, MD[1,3]

[1]School of Medicine and Health Sciences, George Washington University, Washington, DC

[2]School of Engineering and Applied Science, George Washington University, Washington, DC

[3]Department of Orthopaedic Surgery, George Washington University, Washington, DC

ORCID iD for J. Minto: 0000-0002-1517-9870
ORCID iD for X. Zhou: 0000-0002-2930-8514
ORCID iD for J. Osborn: 0000-0002-1013-581X
ORCID iD for L.G. Zhang: 0000-0003-3009-045X
ORCID iD for K. Sarkar: 0000-0003-0701-546X
ORCID iD for R.D. Rao: 0000-0001-9865-8609

References

1. D'Aveni R. The 3-D printing revolution. Harv Bus Rev. 2015;May:40-8.

2. Tack P, Victor J, Gemmel P, Annemans L. 3D-printing techniques in a medical setting: a systematic literature review. Biomed Eng Online. 2016 Oct 21;15(1):115.

3. Trauner KB. The emerging role of 3D printing in arthroplasty and orthopedics. J Arthroplasty. 2018 Aug;33(8):2352-4. Epub 2018 Feb 16.

4. Mulford JS, Babazadeh S, Mackay N. Three-dimensional printing in orthopaedic surgery: review of current and future applications. ANZ J Surg. 2016 Sep;86(9):648-53. Epub 2016 Apr 12.

5. Mumith A, Thomas M, Shah Z, Coathup M, Blunn G. Additive manufacturing: current concepts, future trends. Bone Joint J. 2018 Apr 1;100-B(4):455-60.

6. Mumith A, Coathup M, Chimutengwende-Gordon M, Aston W, Briggs T, Blunn G. Augmenting the osseointegration of endoprostheses using laser-sintered porous collars: an in vivo study. Bone Joint J. 2017 Feb; 99-B(2):276-82.

7. Imanishi J, Choong PF. Three-dimensional printed calcaneal prosthesis following total calcanectomy. Int J Surg Case Rep. 2015;10: 83-7. Epub 2015 Mar 10.

8. Mironov V, Reis N, Derby B. Review: bioprinting: a beginning. Tissue Eng. 2006 Apr; 12(4):631-4.

9. Wang X, Xu S, Zhou S, Xu W, Leary M, Choong P, Qian M, Brandt M, Xie YM. Topological design and additive manufacturing of porous metals for bone scaffolds and orthopaedic implants: a review. Biomaterials. 2016 Mar;83:127-41. Epub 2016 Jan 6.

10. Savio G, Rosso S, Meneghello R, Concheri G. Geometric modeling of cellular materials for additive manufacturing in biomedical field: a review. Appl Bionics Biomech. 2018 Feb 1;2018: 1654782.

11. Bishop ES, Mostafa S, Pakvasa M, Luu HH, Lee MJ, Wolf JM, Ameer GA, He TC, Reid RR. 3-D bioprinting technologies in tissue engineering and regenerative medicine: current and future trends. Genes Dis. 2017 Dec;4(4):185-95. Epub 2017 Nov 22.

12. Papagelopoulos PJ, Savvidou OD, Koutsouradis P, Chloros GD, Bolia IK, Sakellariou VI, Kontogeorgakos VA, Mavrodontis II, Mavrogenis AF, Diamantopoulos P. Three-dimensional technologies in orthopedics. Orthopedics. 2018 Jan 1;41(1):12-20.

13. Guo T, Lembong J, Zhang LG, Fisher JP. Three-dimensional printing articular cartilage: recapitulating the complexity of native tissue. Tissue Eng Part B Rev. 2017 Jun;23(3):225-36. Epub 2016 Dec 27.

14. Schuurman W, Klein TJ, Dhert WJ, van Weeren PR, Hutmacher DW, Malda J. Cartilage regeneration using zonal chondrocyte subpopulations: a promising approach or an over-complicated strategy? J Tissue Eng Regen Med. 2015 Jun;9(6):669-78. Epub 2012 Nov 8.

15. Rankin TM, Wormer BA, Miller JD, Giovinco NA, Al Kassis S, Armstrong DG. Image once, print thrice? Three-dimensional printing of replacement parts. Br J Radiol. 2018 Feb;91(1083): 20170374. Epub 2018 Jan 31.

16. Mitsouras D, Liacouras P, Imanzadeh A, Giannopoulos AA, Cai T, Kumamaru KK, George E, Wake N, Caterson EJ, Pomahac B, Ho VB, Grant GT, Rybicki FJ. Medical 3D printing for the radiologist. Radiographics. 2015 Nov-Dec;35(7): 1965-88.

17. Teo EY, Ong SY, Chong MSK, Zhang Z, Lu J, Moochhala S, Ho B, Teoh SH. Polycaprolactone-based fused deposition modeled mesh for delivery of antibacterial agents to infected wounds. Biomaterials. 2011 Jan;32(1):279-87. Epub 2010 Sep 26.

18. Xu N, Ye X, Wei D, Zhong J, Chen Y, Xu G, He D. 3D artificial bones for bone repair prepared by computed tomography-guided fused deposition modeling for bone repair. ACS Appl Mater Interfaces. 2014 Sep 10;6(17):14952-63. Epub 2014 Aug 22.

19. You F, Wu X, Zhu N, Lei M, Eames BF, Chen X 3rd. Printing of porous cell-laden hydrogel constructs for potential applications in cartilage tissue engineering. ACS Biomater Sci Eng. 2016; 2(7):1200-10.

20. Colosi C, Shin SR, Manoharan V, Massa S, Costantini M, Barbetta A, Dokmeci MR, Dentini M, Khademhosseini A. microfluidic bioprinting of heterogeneous 3D tissue constructs using low-viscosity bioink. Adv Mater. 2016 Jan 27; 28(4):677-84. Epub 2015 Nov 26.

21. Zhang AP, Qu X, Soman P, Hribar KC, Lee JW, Chen S, He S. Rapid fabrication of complex 3D extracellular microenvironments by dynamic optical projection stereolithography. Adv Mater. 2012 Aug 16;24(31):4266-70. Epub 2012 Jul 12.

22. Zhou X, Zhu W, Nowicki M, Miao S, Cui H, Holmes B, Glazer RI, Zhang LG 3rd. Bioprinting a cell-laden bone matrix for breast cancer metastasis study. ACS Appl Mater Interfaces. 2016 Nov 9;8(44):30017-26. Epub 2016 Oct 28.

23. Zhou X, Esworthy T, Lee SJ, Miao S, Cui H, Plesiniak M, Fenniri H, Webster T, Rao RD, Zhang LG 3rd. Printed scaffolds with hierarchical biomimetic structure for osteochondral regeneration. Nanomedicine (Lond). 2019 Jul; 19:58-70. Epub 2019 Apr 18.

24. Zhou X, Cui H, Nowicki M, Miao S, Lee SJ, Masood F, Harris BT, Zhang LG. Three-dimensional-bioprinted dopamine-based matrix for promoting neural regeneration. ACS Appl Mater Interfaces. 2018 Mar 14;10(10): 8993-9001. Epub 2018 Mar 1.

25. Ciocca L, Fantini M, De Crescenzio F, Corinaldesi G, Scotti R. Direct metal laser sintering (DMLS) of a customized titanium mesh for prosthetically guided bone regeneration of atrophic maxillary arches. Med Biol Eng Comput. 2011 Nov;49(11):1347-52. Epub 2011 Jul 21.

26. Mangano F, Bazzoli M, Tettamanti L, Farronato D, Maineri M, Macchi A, Mangano C. Custom-made, selective laser sintering (SLS) blade implants as a non-conventional

solution for the prosthetic rehabilitation of extremely atrophied posterior mandible. Lasers Med Sci. 2013 Sep;28(5):1241-7. Epub 2012 Sep 14.

27. Xia Y, Zhou P, Cheng X, Xie Y, Liang C, Li C, Xu S. Selective laser sintering fabrication of nano-hydroxyapatite/poly-ε-caprolactone scaffolds for bone tissue engineering applications. Int J Nanomedicine. 2013;8:4197-213. Epub 2013 Nov 1.

28. Pataky K, Braschler T, Negro A, Renaud P, Lutolf MP, Brugger J. Microdrop printing of hydrogel bioinks into 3D tissue-like geometries. Adv Mater. 2012 Jan 17;24(3):391-6. Epub 2011 Dec 12.

29. Kuang M, Wang L, Song Y. Controllable printing droplets for high-resolution patterns. Adv Mater. 2014 Oct 29;26(40):6950-8. Epub 2014 Mar 31.

30. Gungor-Ozkerim PS, Inci I, Zhang YS, Khademhosseini A, Dokmeci MR. Bioinks for 3D bioprinting: an overview. Biomater Sci. 2018 May 1;6(5):915-46.

31. Gopinathan J, Noh I. Recent trends in bioinks for 3D printing. Biomater Res. 2018 Apr 6;22:11.

32. Mouser VHM, Levato R, Bonassar LJ, D'Lima DD, Grande DA, Klein TJ, Saris DBF, Zenobi-Wong M, Gawlitta D, Malda J. Three-dimensional bioprinting and its potential in the field of articular cartilage regeneration. Cartilage. 2017 Oct;8(4):327-40. Epub 2016 Sep 1.

33. Stichler S, Böck T, Paxton N, Bertlein S, Levato R, Schill V, Smolan W, Malda J, Teßmar J, Blunk T, Groll J. Double printing of hyaluronic acid/poly(glycidol) hybrid hydrogels with poly(ε-caprolactone) for MSC chondrogenesis. Biofabrication. 2017 Nov 14;9(4):044108.

34. Ng WL, Yeong WY, Naing MW. Polyvinylpyrrolidone-based bio-ink improves cell viability and homogeneity during drop-on-demand printing. Materials (Basel). 2017 Feb 16;10(2):E190.

35. Zadpoor AA, Hedayati R. Analytical relationships for prediction of the mechanical properties of additively manufactured porous biomaterials. J Biomed Mater Res A. 2016 Dec; 104(12):3164-74. Epub 2016 Aug 23.

36. El-Hajje A, Kolos EC, Wang JK, Maleksaeedi S, He Z, Wiria FE, Choong C, Ruys AJ. Physical and mechanical characterisation of 3D-printed porous titanium for biomedical applications. J Mater Sci Mater Med. 2014 Nov;25(11):2471-80. Epub 2014 Jul 23.

37. Bose S, Roy M, Bandyopadhyay A. Recent advances in bone tissue engineering scaffolds. Trends Biotechnol. 2012 Oct;30(10):546-54. Epub 2012 Aug 30.

38. Derakhshanfar S, Mbeleck R, Xu K, Zhang X, Zhong W, Xing M. 3D bioprinting for biomedical devices and tissue engineering: a review of recent trends and advances. Bioact Mater. 2018 Feb 20;3(2):144-56.

39. Karageorgiou V, Kaplan D. Porosity of 3D biomaterial scaffolds and osteogenesis. Biomaterials. 2005 Sep;26(27):5474-91.

40. Schuurman W, Harimulyo EB, Gawlitta D, Woodfield TB, Dhert WJ, van Weeren PR, Malda J. Three-dimensional assembly of tissue-engineered cartilage constructs results in cartilaginous tissue formation without retainment of zonal characteristics. J Tissue Eng Regen Med. 2016 Apr;10(4):315-24. Epub 2013 Apr 18.

41. Jinnai H, Nishikawa Y, Ito M, Smith SD, Agard DA, Spontak RJ. Topological similarity of sponge-like bicontinuous morphologies differing in length scale. Adv Mater. 2002;14(22): 1615-8.

42. Bobbert FSL, Lietaert K, Eftekhari AA, Pouran B, Ahmadi SM, Weinans H, Zadpoor AA. Additively manufactured metallic porous biomaterials based on minimal surfaces: a unique combination of topological, mechanical, and mass transport properties. Acta Biomater. 2017 Apr 15;53:572-84. Epub 2017 Feb 16.

43. Honigmann P, Sharma N, Okolo B, Popp U, Msallem B, Thieringer FM. Patient-specific surgical implants made of 3D printed PEEK: material, technology, and scope of surgical application. BioMed Res Int. 2018 Mar 19;2018: 4520636.

44. Ma R, Tang T. Current strategies to improve the bioactivity of PEEK. Int J Mol Sci. 2014 Mar 28;15(4):5426-45.

45. Li CS, Vannabouathong C, Sprague S, Bhandari M. The use of carbon-fiber-reinforced (CFR) PEEK material in orthopedic implants: a systematic review. Clin Med Insights Arthritis Musculoskelet Disord. 2015 Feb 23;8:33-45.

46. Abdullah MR, Goharian A, Abdul Kadir MR, Wahit MU. Biomechanical and bioactivity concepts of polyetheretherketone composites for use in orthopedic implants-a review. J Biomed Mater Res A. 2015 Nov;103(11):3689-702. Epub 2015 Apr 28.

47. Armstrong JP, Burke M, Carter BM, Davis SA, Perriman AW. 3D bioprinting using a templated porous bioink. Adv Healthc Mater. 2016 Jul; 5(14):1724-30. Epub 2016 Jun 22.

48. Kang HW, Lee SJ, Ko IK, Kengla C, Yoo JJ, Atala A. A 3D bioprinting system to produce human-scale tissue constructs with structural integrity. Nat Biotechnol. 2016 Mar;34(3):312-9. Epub 2016 Feb 15.

49. Cui H, Zhu W, Nowicki M, Zhou X, Khademhosseini A, Zhang LG. Hierarchical fabrication of engineered vascularized bone biphasic constructs via dual 3D bioprinting: integrating regional bioactive factors into architectural design. Adv Healthc Mater. 2016 Sep;5(17):2174-81. Epub 2016 Jul 7.

50. Holmes B, Bulusu K, Plesniak M, Zhang LG. A synergistic approach to the design, fabrication and evaluation of 3D printed micro and nano featured scaffolds for vascularized bone tissue repair. Nanotechnology. 2016 Feb 12;27(6): 064001. Epub 2016 Jan 13.

51. Cui H, Zhu W, Holmes B, Zhang LG. Biologically inspired smart release system based on 3D bioprinted perfused scaffold for vascularized tissue regeneration. Adv Sci (Weinh). 2016 Apr 15;3(8):1600058.

52. Heo DN, Castro NJ, Lee SJ, Noh H, Zhu W, Zhang LG. Enhanced bone tissue regeneration using a 3D printed microstructure incorporated with a hybrid nano hydrogel. Nanoscale. 2017 Apr 20;9(16):5055-62.

53. Zhang L, Hu J, Athanasiou KA. The role of tissue engineering in articular cartilage repair and regeneration. Crit Rev Biomed Eng. 2009; 37(1-2):1-57.

54. Bekkers JE, Tsuchida AI, van Rijen MH, Vonk LA, Dhert WJ, Creemers LB, Saris DB. Single-stage cell-based cartilage regeneration using a combination of chondrons and mesenchymal stromal cells: comparison with microfracture. Am J Sports Med. 2013 Sep;41(9):2158-66. Epub 2013 Jul 5.

55. Poole CA, Ayad S, Schofield JR. Chondrons from articular cartilage: I. Immunolocalization of type VI collagen in the pericellular capsule of isolated canine tibial chondrons. J Cell Sci. 1988 Aug;90(Pt 4):635-43.

56. Zhang Z. Chondrons and the pericellular matrix of chondrocytes. Tissue Eng Part B Rev. 2015 Jun;21(3):267-77. Epub 2014 Dec 16.

57. Dominici M, Le Blanc K, Mueller I, Slaper-Cortenbach I, Marini F, Krause D, Deans R, Keating A, Prockop Dj, Horwitz E. Minimal criteria for defining multipotent mesenchymal stromal cells. The International Society for Cellular Therapy position statement. Cytotherapy. 2006;8(4):315-7.

58. Acharya C, Adesida A, Zajac P, Mumme M, Riesle J, Martin I, Barbero A. Enhanced chondrocyte proliferation and mesenchymal stromal cells chondrogenesis in coculture pellets mediate improved cartilage formation. J Cell Physiol. 2012 Jan;227(1):88-97.

59. Mo XT, Guo SC, Xie HQ, Deng L, Zhi W, Xiang Z, Li XQ, Yang ZM. Variations in the ratios of co-cultured mesenchymal stem cells and chondrocytes regulate the expression of cartilaginous and osseous phenotype in alginate constructs. Bone. 2009 Jul;45(1):42-51. Epub 2008 Jul 29.

60. de Windt TS, Saris DB, Slaper-Cortenbach IC, van Rijen MH, Gawlitta D, Creemers LB, de Weger RA, Dhert WJ, Vonk LA. Direct cell-cell contact with chondrocytes is a key mechanism in multipotent mesenchymal stromal cell-mediated chondrogenesis. Tissue Eng Part A. 2015 Oct;21(19-20):2536-47. Epub 2015 Aug 12.

61. Jiang Y, Tuan RS. Origin and function of cartilage stem/progenitor cells in osteoarthritis. Nat Rev Rheumatol. 2015 Apr;11(4):206-12. Epub 2014 Dec 23.

62. Vermonden T, Censi R, Hennink WE. Hydrogels for protein delivery. Chem Rev. 2012 May 9;112(5):2853-88. Epub 2012 Feb 23.

63. Zhou X, Nowicki M, Cui H, Zhu W, Fang X, Miao S, Lee S, Keidar M, Zhang LG. 3D bioprinted graphene oxide-incorporated matrix for promoting chondrogenic differentiation of human bone marrow mesenchymal stem cells. Carbon. 2017;116:615-24.

64. Nowicki MA, Castro NJ, Plesniak MW, Zhang LG. 3D printing of novel osteochondral scaffolds with graded microstructure. Nanotechnology. 2016 Oct 14;27(41): 414001. Epub 2016 Sep 8.

65. Castro NJ, O'Brien J, Zhang LG. Integrating biologically inspired nanomaterials and table-top stereolithography for 3D printed biomimetic osteochondral scaffolds. Nanoscale. 2015 Sep 7;7(33):14010-22. Epub 2015 Aug 3.

66. Castro NJ, Patel R, Zhang LG. Design of a novel 3D printed bioactive nanocomposite scaffold for improved osteochondral regeneration. Cell Mol Bioeng. 2015 Sep;8(3):416-32.

67. Holmes B, Zhu W, Li J, Lee JD, Zhang LG. Development of novel three-dimensional printed scaffolds for osteochondral regeneration. Tissue Eng Part A. 2015 Jan;21(1-2):403-15. Epub 2014 Sep 12.

68. Heckman JD, Ryaby JP, McCabe J, Frey JJ, Kilcoyne RF. Acceleration of tibial fracture-healing by non-invasive, low-intensity pulsed ultrasound. J Bone Joint Surg Am. 1994 Jan; 76(1):26-34.

69. Azuma Y, Ito M, Harada Y, Takagi H, Ohta T, Jingushi S. Low-intensity pulsed ultrasound accelerates rat femoral fracture healing by acting on the various cellular reactions in the

fracture callus. J Bone Miner Res. 2001 Apr;16(4): 671-80.

70. Hantes ME, Mavrodontidis AN, Zalavras CG, Karantanas AH, Karachalios T, Malizos KN. Low-intensity transosseous ultrasound accelerates osteotomy healing in a sheep fracture model. J Bone Joint Surg Am. 2004 Oct;86(10):2275-82.

71. Katiyar A, Duncan RL, Sarkar K. Ultrasound stimulation increases proliferation of MC3T3-E1 preosteoblast-like cells. J Ther Ultrasound. 2014 Jan 2;2:1.

72. Byl NN, McKenzie A, Wong T, West J, Hunt TK. Incisional wound healing: a controlled study of low and high dose ultrasound. J Orthop Sports Phys Ther. 1993 Nov;18(5):619-28.

73. Silverman RH, Vogelsang B, Rondeau MJ, Coleman DJ. Therapeutic ultrasound for the treatment of glaucoma. Am J Ophthalmol. 1991 Mar 15;111(3):327-37.

74. Lim K, Kim J, Seonwoo H, Park SH, Choung PH, Chung JH. In vitro effects of low-intensity pulsed ultrasound stimulation on the osteogenic differentiation of human alveolar bone-derived mesenchymal stem cells for tooth tissue engineering. BioMed Res Int. 2013;2013: 269724. Epub 2013 Sep 30.

75. Zhou X, Castro NJ, Zhu W, Cui H, Aliabouzar M, Sarkar K, Zhang LG. Improved human bone marrow mesenchymal stem cell osteogenesis in 3D bioprinted tissue scaffolds with low intensity pulsed ultrasound stimulation. Sci Rep. 2016 Sep 6;6:32876.

76. Aliabouzar M, Lee SJ, Zhou X, Zhang GL, Sarkar K. Effects of scaffold microstructure and low intensity pulsed ultrasound on chondrogenic differentiation of human mesenchymal stem cells. Biotechnol Bioeng. 2018 Feb;115(2):495-506. Epub 2017 Nov 22.

77. Sarkar K, Shi WT, Chatterjee D, Forsberg F. Characterization of ultrasound contrast microbubbles using in vitro experiments and viscous and viscoelastic interface models for encapsulation. J Acoust Soc Am. 2005 Jul; 118(1):539-50.

78. Paul S, Nahire R, Mallik S, Sarkar K. Encapsulated microbubbles and echogenic liposomes for contrast ultrasound imaging and targeted drug delivery. Comput Mech. 2014 Mar;53(3):413-35.

79. Kumar KN, Sarkar K. Interfacial rheological properties of contrast microbubble Targestar P as a function of ambient pressure. Ultrasound Med Biol. 2016 Apr;42(4):1010-7. Epub 2016 Jan 6.

80. Paul S, Katiyar A, Sarkar K, Chatterjee D, Shi WT, Forsberg F. Material characterization of the encapsulation of an ultrasound contrast microbubble and its subharmonic response: strain-softening interfacial elasticity model. J Acoust Soc Am. 2010 Jun;127(6):3846-57.

81. Chatterjee D, Sarkar K. A Newtonian rheological model for the interface of microbubble contrast agents. Ultrasound Med Biol. 2003 Dec;29(12):1749-57.

82. Aliabouzar M, Zhang LG, Sarkar K. Lipid coated microbubbles and low intensity pulsed ultrasound enhance chondrogenesis of human mesenchymal stem cells in 3D printed scaffolds. Sci Rep. 2016 Nov 24;6:37728.

83. Osborn J, Aliabouzar M, Zhou X, Rao R, Zhang LG, Sarkar K. Enhanced osteogenic differentiation of human mesenchymal stem cells using microbubbles and low intensity pulsed ultrasound on 3D printed scaffolds. Adv Biosys. 2019;3(2):1800257.

84. Evans NT, Irvin CW, Safranski DL, Gall K. Impact of surface porosity and topography on the mechanical behavior of high strength biomedical polymers. J Mech Behav Biomed Mater. 2016 Jun;59:459-73. Epub 2016 Mar 4.

85. Razavi SMJ, Bordonaro GG, Ferro P, Torgersen J, Berto F. Fatigue behavior of porous Ti-6Al-4V made by laser-engineered net shaping. Materials (Basel). 2018 Feb 12; 11(2):E284.

86. ASTM International. ASTM F1472 - 14. Accessed 2019 Jul 9. https://www.astm.org/Standards/F1472.htm

87. Slotwinski J, Cooke A, Moylan S. 2012. Mechanical properties testing for metal parts made via additive manufacturing. National Institute of Standards and Technology Internal Report (NISTIR). Report 7847.

88. U.S. Food and Drug Administration. CFR - Code of Federal Regulations Title 21. 2018. Accessed 2019 Sep 12. https://www.accessdata.fda.gov/scripts/cdrh/cfdocs/cfcfr/CFRSearch.cfm?CFRPart=888&showFR=1

89. Sterling A, Shamsaei N, Torries B, Thompson SM. Fatigue behaviour of additively manufactured Ti-6Al-4V. Procedia Eng. 2015;133:576-89.

90. Hinderdael M, Strantza M, De Baere D, Devesse W, De Graeve I, Terryn H, Guillaume P. Fatigue performance of Ti-6Al-4V additively manufactured specimens with integrated capillaries of an embedded structural health monitoring system. Materials (Basel). 2017 Aug 25;10(9):E993.

91. Carli AV, Warth LC, de Mesy Bentley KL, Nestor BJ. Short to midterm follow-up of the Tritanium primary acetabular component: a cause for concern. J Arthroplasty. 2017 Feb; 32(2):463-9. Epub 2016 Aug 8.

92. Yoshioka S, Nakano S, Kinoshita Y, Nakamura M, Goto T, Hamada D, Sairyo K. Comparison of a highly porous titanium cup (Tritanium) and a conventional hydroxyapatite-coated porous titanium cup: a retrospective analysis of clinical and radiological outcomes in hip arthroplasty among Japanese patients. J Orthop Sci. 2018 Nov;23(6):967-72. Epub 2018 Jul 25.

93. Bagaria V, Chaudhary K. A paradigm shift in surgical planning and simulation using 3Dgraphy: experience of first 50 surgeries done using 3D-printed biomodels. Injury. 2017 Nov; 48(11):2501-8. Epub 2017 Sep 1.

94. Radermacher K, Portheine F, Anton M, Zimolong A, Kaspers G, Rau G, Staudte HW. Computer assisted orthopaedic surgery with image based individual templates. Clin Orthop Relat Res. 1998 Sep;(354):28-38.

95. Henckel J, Holme TJ, Radford W, Skinner JA, Hart AJ. 3D-printed patient-specific guides for hip arthroplasty. J Am Acad Orthop Surg. 2018 Aug 15;26(16):e342-8.

96. Kunz M, Rudan JF, Xenoyannis GL, Ellis RE. Computer-assisted hip resurfacing using individualized drill templates. J Arthroplasty. 2010 Jun;25(4):600-6. Epub 2009 May 22.

97. Gauci MO, Boileau P, Baba M, Chaoui J, Walch G. Patient-specific glenoid guides provide accuracy and reproducibility in total shoulder arthroplasty. Bone Joint J. 2016 Aug; 98-B(8):1080-5.

98. Roner S, Carrillo F, Vlachopoulos L, Schweizer A, Nagy L, Fuernstahl P. Improving accuracy of opening-wedge osteotomies of distal radius using a patient-specific ramp-guide technique. BMC Musculoskelet Disord. 2018 Oct 15;19(1):374.

99. Huang H, Hsieh MF, Zhang G, Ouyang H, Zeng C, Yan B, Xu J, Yang Y, Wu Z, Huang W. Improved accuracy of 3D-printed navigational template during complicated tibial plateau fracture surgery. Australas Phys Eng Sci Med. 2015 Mar;38(1):109-17. Epub 2015 Feb 7.

100. Sha Y, Wang H, Ding J, Tang H, Li C, Luo H, Liu J, Xu Y. A novel patient-specific navigational template for anatomical reconstruction of the lateral ankle ligaments. Int Orthop. 2016 Jan; 40(1):59-64. Epub 2015 Jul 2.

101. Arnal-Burró J, Pérez-Mañanes R, Gallo-Del-Valle E, Igualada-Blazquez C, Cuervas-Mons M, Vaquero-Martín J. Three dimensional-printed patient-specific cutting guides for femoral varization osteotomy: do it yourself. Knee. 2017 Dec;24(6):1359-68. Epub 2017 Oct 1.

102. Volpi P, Prospero E, Bait C, Cervellin M, Quaglia A, Redaelli A, Denti M. High accuracy in knee alignment and implant placement in unicompartmental medial knee replacement when using patient-specific instrumentation. Knee Surg Sports Traumatol Arthrosc. 2015 May;23(5):1292-8. Epub 2013 Dec 4.

103. Dao Trong ML, Diezi C, Goerres G, Helmy N. Improved positioning of the tibial component in unicompartmental knee arthroplasty with patient-specific cutting blocks. Knee Surg Sports Traumatol Arthrosc. 2015 Jul;23(7): 1993-8. Epub 2014 Jan 17.

104. Guo F, Dai J, Zhang J, Ma Y, Zhu G, Shen J, Niu G. Individualized 3D printing navigation template for pedicle screw fixation in upper cervical spine. PLoS One. 2017 Feb 2;12(2): e0171509.

105. Bundoc RC, Delgado GG, Grozman SA. A novel patient-specific drill guide template for pedicle screw insertion into the subaxial cervical spine utilizing stereolithographic modelling: an in vitro study. Asian Spine J. 2017 Feb;11(1):4-14. Epub 2017 Feb 17.

106. Cho W, Job AV, Chen J, Baek JH. A review of current clinical applications of three-dimensional printing in spine surgery. Asian Spine J. 2018 Feb;12(1):171-7. Epub 2018 Feb 7.

107. Stryker. Stryker's Spine Division receives FDA clearance for 3D-printed Tritanium TL curved posterior lumbar cage. Accessed 2019 Sep 12. https://www.stryker.com/us/en/about/news/2018/stryker_s-spine-division-receives-fda-clearance-for-3d-printed-t.html

108. Wang B, Hao Y, Pu F, Jiang W, Shao Z. Computer-aided designed, three dimensional-printed hemipelvic prosthesis for peri-acetabular malignant bone tumour. Int Orthop. 2018 Mar; 42(3):687-94. Epub 2017 Sep 27.

109. Xu N, Wei F, Liu X, Jiang L, Cai H, Li Z, Yu M, Wu F, Liu Z. Reconstruction of the upper cervical spine using a personalized 3D-printed vertebral body in an adolescent with Ewing sarcoma. Spine. 2016 Jan;41(1):E50-4.

110. Mao Y, Xu C, Xu J, Li H, Liu F, Yu D, Zhu Z. The use of customized cages in revision total hip arthroplasty for Paprosky type III acetabular bone defects. Int Orthop. 2015 Oct;39(10): 2023-30. Epub 2015 Aug 19.

111. Faizan A, Bhowmik-Stoker M, Alipit V, Kirk AE, Krebs VE, Harwin SF, Meneghini RM. Development and verification of novel porous titanium metaphyseal cones for revision total knee arthroplasty. J Arthroplasty. 2017 Jun; 32(6):1946-53. Epub 2017 Jan 18.

112. Arabnejad S, Johnston B, Tanzer M, Pasini D. Fully porous 3D printed titanium femoral

stem to reduce stress-shielding following total hip arthroplasty. J Orthop Res. 2017 Aug;35(8):1774-83. Epub 2016 Oct 4.

113. Honigmann P, Schumacher R, Marek R, Büttner F, Thieringer F, Haefeli M. A three-dimensional printed patient-specific scaphoid replacement: a cadaveric study. J Hand Surg Eur Vol. 2018 May;43(4):407-12. Epub 2018 Feb 16.

114. U.S. Department of Health & Human Services. Technical considerations for additive manufactured devices: guidance for industry and Food and Drug Administration staff. 2017. Accessed 2019 Sep 12. https://www.fda.gov/files/medical%20devices/published/Technical-Considerations-for-Additive-Manufactured-Medical-Devices—Guidance-for-Industry-and-Food-and-Drug-Administration-Staff.pdf

115. Saunders S. Additive Orthopaedics receives 510(k) clearance for patient specific 3D printed bone segments. 2018. Accessed 2019 Sep 12. https://3dprint.com/214299/additive-orthopaedics-3d-bone/

116. Scott C. Zimmer Biomet's first 3D printed spinal implants receive FDA clearance. 2018. Accessed 2019 Sep 12. https://3dprint.com/214860/zimmer-biomet-spinal-implants/

117. U.S. Department of Health & Human Services. Food and Drug Administration: Custom Device Exemption. 2014. Accessed 2019 Sep 12. https://www.fda.gov/downloads/Training/CDRHLearn/UCM418838.pdf

118. BlueCross BlueShield of North Carolina. Corporate medical policy: three dimensional printed orthopedic implants. 2018. Accessed 2019 Sep 12. https://www.bluecrossnc.com/sites/default/files/document/attachment/services/public/pdfs/medicalpolicy/three_dimensional_printed_orthopedic_implants.pdf

119. Stryker. Tritanium® manufacturing overview. 2016. Accessed 2019 Sep 12. https://www.stryker.com/builttofuse/media/assets/TRITA-BR-2 Tritanium Manufacturing Overview FINAL.pdf

120. Stryker. Technical summary: Tritanium® PL Posterior Lumbar Cage. 2017. Accessed 2019 Aug 12. http://az621074.vo.msecnd.net/syk-mobile-content-cdn/global-content-system/SYKGCSDOC-2-43623/fiyA_cRJtqVDK-G5V9IWiFXONJbJwg/TRITA_BR_3.pdf

121. Stryker.Tritanium C. 2018. Accessed 2019 Sep 12. https://www.stryker.com/us/en/spine/products/tritanium-c.html

122. Kavlock KD. FDA traditional 510(k) Premarket Notification. 2017. Accessed 2019 Sep 12. https://www.accessdata.fda.gov/cdrh_docs/pdf17/K171496.pdf

123. Stryker. Triathlon Tritanium® Total Knee System clinical evidence. 2019. Accessed 2019 Sep 12. http://az621074.vo.msecnd.net/syk-mobile-content-cdn/global-content-system/SYKGCSDOC-2-48507/PgzCOh5946NVMmIjTuBlaWGxQkxmhw/TRIATH_BRO_13.pdf

124. Keith EI. 510(k) summary. 2013. Accessed 2019 Sep 12. https://www.accessdata.fda.gov/cdrh_docs/pdf12/K122770.pdf

125. Jackson B. Zimmer Biomet introduces first 3D printed spinal implant to market. 2018. Accessed 2019 Sep 12. https://3dprintingindustry.com/news/zimmer-biomet-introduces-first-3d-printed-spinal-implant-market-133727/

126. Emerging Implant Technologies. EIT Cervical Cage. Accessed 2019 Sep 12. https://innosurge.com/sites/default/files/uploads/product-documents/Operationsvejledning til delaftale 12-EIT Cervikal cage.pdf

127. Eggleton J. FDA 510(k) summary. 2017. Accessed 2019 Oct 17. https://www.accessdata.fda.gov/cdrh_docs/pdf17/K172888.pdf

128. Centinel Spine. For STALIF®, STALIF C®, STALIF C-Ti™, STALIF M™, STALIF M-Ti™, STALIF L™, ALTOS™ PCT, and STALIF MIDLINE®. Accessed 2019 Sep 12. https://www.centinelspine.com/corp_flx.php

129. Melkerson MN. FDA 510(k) summary. 2018. Accessed 2019 Sep 12. https://www.accessdata.fda.gov/cdrh_docs/pdf17/K173347.pdf

130. Exactech. Revision Acetabular System. Accessed 2019 Sep 12. https://www.exac.com/hip/novation-integrip/

131. Melkerson M. FDA 510(k) summary. 2010. Accessed 2019 Sep 12. https://www.accessdata.fda.gov/cdrh_docs/pdf10/K101761.pdf

132. Camber Spine. SPIRA®-C open matrix cervical interbody. Accessed 2019 Sep 12. https://www.cambermedtech.com/spirac

133. Camber Spine. ENZA®-A titanium ALIF. Accessed 2019 Sep 12. https://www.cambermedtech.com/enzaa-titanium-alif

134. Boissonneault T. Additive Orthopaedics takes step ahead with FDA-approved 3D printed locking lattice plates. 2019. Accessed 2019 Sep 12. https://www.3dprintingmedia.network/additive-orthopaedics-fda-approval

135. Additive Orthopaedics. Our products. Accessed 2019 Sep 12. https://www.additiveorthopaedics.com/our-products/

136. Ali S. FDA 510(k) summary. 2019. Accessed 2019 Sep 12. https://www.accessdata.fda.gov/cdrh_docs/pdf18/K183011.pdf

137. Melkerson MN. FDA 510(k) summary. 2016. Accessed 2019 Sep 12. https://www.accessdata.fda.gov/cdrh_docs/pdf15/K153207.pdf

138. Melkerson MN. FDA 510(k) summary. 2017. Accessed 2019 Sep 12. https://www.accessdata.fda.gov/cdrh_docs/pdf16/K162733.pdf

139. Clarke C. FDA clears 3D printed titanium medical implant for use. 2017 Accessed 2019 Sep 12. https://3dprintingindustry.com/news/fda-clears-3d-printed-titanium-medical-implant-use-115880/